JOURNAL OF CATALYSIS 119, 342–353 (1989)

Methanol Adsorption and Decomposition on Rhodium

G.-K. CHUAH,[1] N. KRUSE, W. A. SCHMIDT, J. H. BLOCK, AND G. ABEND

Fritz-Haber-Institut der Max-Planck-Gesellschaft, Faradayweg 4-6, D-1000 Berlin 33, Federal Republic of Germany

Received February 15, 1989; revised May 12, 1989

The decomposition of methanol on rhodium probed from ~200 atomic sites of the (001) or (111) planes of Rh field emitter crystals but randomly with regard to crystallographic zones was studied by pulsed field desorption mass spectrometry. High electric field pulses were used to quantitatively desorb the final products, carbon monoxide and hydrogen, thus achieving steady-state conditions. Substantial amounts of methoxy (mainly desorbed as CH_3^+ ions) were also present at the surface. Applying a steady electric field, $F_R \geqq 4$ V/nm, between the field pulses, led to a deceleration of the decomposition reaction and to an increase of the amount of adsorbed CH_3O and CH_2O species. There were indications that the rate-determining step of the reaction is C–H bond cleavage in adsorbed methoxy to form the CH_2O intermediate. This was supported by the observation of a kinetic isotope effect in the formation of CD_2O and CHDO from methyl-d_2-alcohol, CHD_2OH. Here, the C–H bond breaking to form the CD_2O was found to be twice as fast as the breaking of the C–D bond which results in CHDO. Field ion microscopy was applied to investigate the influence of the reaction on the structure of the whole hemispherical single crystal surface. There were neither topographic changes nor corrosion of the Rh surface after field-free exposure to 2 Pa methanol at temperatures up to 423 K.

1. INTRODUCTION

The catalytic formation of methanol from synthesis gas (CO/H_2) belongs to the economically most important chemical reactions. Catalysts applied industrially are based on the compositions $Cu/ZnO/Cr_2O_3$ and $Cu/ZnO/Al_2O_3$. High activity in the formation of oxygenates was also reported for catalysts containing Pt group metals (*1, 2*). The detailed microscopic mechanism of this reaction is not known. The use of surface analytical tools to study methanol synthesis is hampered by the fact that these tools need ultrahigh vacuum conditions for their proper operation while the synthesis reaction requires the reactants at high pressures. However, the decomposition reaction is not limited by this restriction and, according to the principle of microscopic reversibility, may provide insight into reaction pathways of the synthesis reaction.

Adsorption and decomposition of methanol is expected to be influenced by the surface structure of the catalyst. This influence can be investigated by using single crystal surfaces of well defined orientation. In studies with the more noble transition metals of Group VIII mainly low index planes were probed with surface analytical tools (*3–11*). The decomposition pathways over stepped surfaces of Rh and Ru were studied very recently (*11*). There is general agreement among the various authors that a methoxy species, CH_3O_{ad}, is formed during dissociative adsorption of methanol on these metals (*3–11*). The methoxy species decomposes to carbon monoxide and hydrogen at higher temperatures. On Ru and Rh stepped surfaces, CH_xO_{ad} (x = 1,2) intermediates were detected during the decomposition reaction (*11*). This result suggests gradual hydrogen abstraction from CH_3O_{ad}. Solymosi *et al.* investigated the

[1] Department of Chemistry, National University of Singapore, Kent Ridge, Singapore 0511.

0021-9517/89 $3.00

influence of coadsorbed potassium (*12*) and oxygen (*13*) on methanol adsorption and decomposition on Rh(111). The presence of oxygen on the surface seems to promote CH_3OH dissociation and formation of a methoxy species which undergoes decomposition at 200 K instead of associative desorption as CH_3OH.

The present work is an extension of our previous studies (*11*) and describes decomposition of CH_3O_{ad} as the rate-controlling step in the steady decomposition of methanol on Rh. Both CH_3OH and CHD_2OH are used since the observation of a possible kinetic isotope effect would allow direct identification of the reaction site in the molecule. Pulsed field desorption mass spectrometry (PFDMS) with its ultimate sensitivity is applied to provide time resolved data of the chemical processes occurring at ~200 atomic sites chosen from the central poles of [001]- or [111]-oriented Rh field emitters but due to technical reasons randomly with regard to crystallographic zones. Specimens with radii of ~100 nm or less which are used here can be regarded as excellent models of catalyst particles. Therefore, further studies were directed to field ion microscope (FIM) observations in which after field-free methanol decomposition changes in crystallographic plane sizes can be determined.

2. EXPERIMENTAL

The experimental technique of PFDMS and its applications to kinetic studies of surface reactions have been described in Refs. (*14, 15*). Species adsorbed on a field emitter tip can be desorbed as positively charged ions by high electric field pulses of up to 50 V/nm periodically (≦10 kHz) applied to a counter electrode in front of the emitter. These ions can be identified by time-of-flight mass spectrometry. A channel plate image intensifier allows the determination of the orientation of the emitter with respect to a probe hole. The probe hole selects a few up to 200 atomic sites. By tilting the tip, different crystal areas can be probed and the reaction products of the chosen entities can be investigated.

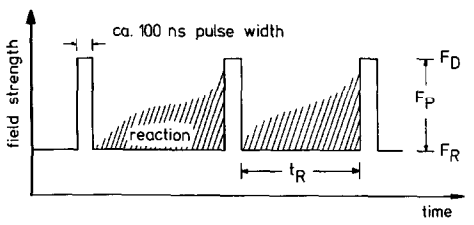

FIG. 1. Schematic diagram of sequentially applied field pulses, F_P. Also, a steady reaction field, F_R, can be applied in the reaction time, t_R. Pulse repetition rates can be varied up to 10 kHz.

Under continuous gas supply, molecules adsorb on the tip surface, where they undergo reactions in the time interval, t_R, between the pulses (Fig. 1). At very high desorption field strengths each pulse removes the whole adsorbed layer from the surface so that the ion intensities represent the concentrations of the corresponding adsorbed species, parent molecules, intermediates, and products, at the end of the time interval t_R. The detected intensities depend on t_R, gas pressure, and surface temperature. The influence of an electric field on the reaction can be investigated by applying a steady field (reaction field), F_R, during the time interval t_R (Fig. 1).

Rhodium tips were prepared from wires (purity 99.9% Goodfellow, 0.12 mm ϕ) by etching in molten $NaCl/NaNO_3$ (1:4 w/w). Tips used in the PFDMS apparatus were cleaned by cycles of heating at 1100 K and field evaporation at 298 K. Emitter temperatures were measured by a Chromel-Alumel thermocouple spot-welded onto the shank of the tip. CH_3OH (E. Merck, p.a. grade) and methyl-d_2 alcohol, CHD_2OH (MSD Isotopes, 98.6 at.% D), were degassed by several freeze–pump–thaw cycles before dosing. Pressure values indicated with the experimental data refer to gauge readings.

FIM experiments were performed in a separate UHV chamber. The tip, after heat treatment to 620 K, was cooled by liquid

nitrogen to 78 K and cleaned by low temperature field evaporation, first in a 20:1 mixture of neon and hydrogen (Messer Griesheim, purity of both gases ≧99.999%) and then in pure neon. The field at the tip surface was adjusted to "best image field" before image photographing. Reaction studies with methanol were carried out field-free and at various temperatures between 295 and 423 K. For this purpose neon was pumped off and an isolation cell was manipulated into position so that it completely sealed off the tip from the rest of the chamber. Methanol was introduced into the isolation cell via a leak valve. After reaction times of 10 min at pressures of up to 2 Pa, methanol was pumped away and the tip cooled again to 78 K. Photographs of the images were taken in neon at increasing field strengths beginning from the first appearance of bright spots up to the onset of field evaporation. "Blind" experiments, i.e., without methanol, were carried out at the various temperatures in order to eliminate any effects due to annealing.

3. RESULTS

3.1. Mass Spectra

Figure 2 shows a time-of-flight mass spectrum that was obtained by probing ~150 atomic sites of the stepped surface region in the vicinity of the (001) pole of the Rh specimen. The spectrum was independent of different crystallographic zones on these atomic steps. A field strength $F_D = 29$ V/nm was found to be sufficient in order to desorb the adsorbed layer quantitatively by the field pulses. Under these conditions, the substrate material already undergoes some field evaporation yielding Rh^{2+} and, in smaller amounts, Rh^+ ions. No steady electric field was applied in the time between the pulses, thus Fig. 2 refers to the field-free reaction of methanol on Rh during a time $t_R = 1$ ms at $T = 298$ K and a gas pressure $p = 1.3 \times 10^{-5}$ Pa.

Figure 2 shows various ionic species, the intensities of which are characteristic for

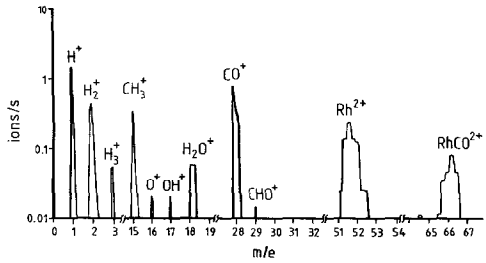

FIG. 2. Mass spectrum of field desorbed ions after CH_3OH had been adsorbed on and reacted with a rhodium surface in the absence of a steady electric field. $F_D = 29$ V/nm, $t_R = 1$ ms, $T = 298$ K, $p = 1.3 \times 10^{-5}$ Pa.

the chosen experimental conditions. The parent species, CH_3OH^+, is desorbed in very small amounts only. The dissociatively adsorbed methoxy is preferentially desorbed as CH_3^+ (see below). High intensities are also observed for H^+, H_2^+, and CO^+. Thus, at 298 K, large amounts of adsorbed CH_3OH molecules decompose toward H_{ad} and CO_{ad}. The occurrence of H_2^+ does not necessarily indicate the presence of molecularly adsorbed hydrogen since during the thermally activated field desorption process H_{ad} may recombine before desorption. CO_{ad} is not only desorbed as CO^+ but also as $RhCO^{2+}$, i.e., under simultaneous removal of a Rh lattice atom. At reaction times longer than 1 ms and/or at higher surface temperatures, $Rh(CO)_x^{2+}$ (x up to 3) species can be observed. The neutral Rh-subcarbonyls are formed during a consecutive surface reaction by successive addition of CO_{ad} to the respective precursor species. Details are discussed elsewhere (*16*).

Besides the educt and product ions, dehydrogenated species, CH_xO^+ ($x = 1$–3), are also desorbed from the adsorbed layer. Their intensities are low in Fig. 2 but increase in the presence of a steady electric field as described below. The detection of dehydrogenated CH_xO^+ species suggests stepwise loss of hydrogen from a methoxy species formed initially during dissociative methanol adsorption. EELS and UPS data

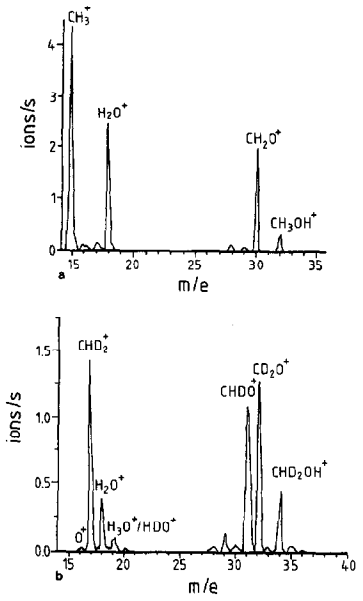

FIG. 3. Mass spectrum of field desorbed ions from (a) CH_3OH and (b) CHD_2OH adsorbed on a Rh tip in the presence of a steady field, $F_R = 4$ V/nm. $F_P = 24$ V/nm, $F_D = 28$ V/nm, $t_R = 250$ μs, $T = 298$ K, $p = 1.3 \times 10^{-5}$ Pa (impingement rate enhanced by F_R).

indicate that this species is bonded to the surface by its oxygen atom (*10*). Field desorption of CH_3O_{ad} may result in either Rh–O or C–O bond breaking so that CH_3O^+ as well as CH_3^+ ions are detected. Figures 2 and 3a show that CH_3^+ ion formation occurs with much higher probability than CH_3O^+ formation. After desorption of CH_3^+, oxygen is left at the surface. However, it does not accumulate but is field desorbed after reaction with H_{ad}, mainly as H_2O^+ and in smaller amounts as OH^+ and O^+ (termed collectively as H_yO^+ below). The formation of H_2O_{ad} from hydrogen and oxygen adsorbed on Rh surfaces is well known from other studies (*13, 17*). By reasons of stoichiometry we expect the intensity sum, $\Sigma_y H_y O^+$, to be equal to the CH_3^+ intensity. The apparent deficiency of H_yO^+ ions, however, is not surprising, since part of the H_2O_{ad} formed can desorb thermally during the time interval, $t_R = 1$ ms, at $T = 298$ K. This is supported by TPD studies of other authors (*13, 17, 18*). The adsorption of water on Rh (111) (*18*) and the reaction of hydrogen and oxygen on Rh (100) (*17*) resulted in desorption peak temperatures of $T = 191$ K (*18*) and $T = 240$ K (*17*). Solymosi *et al.* (*13*) found water peak temperatures of $T = 184$ K and $T = 279$ K after the reaction of CH_3OH with oxygen-precovered ($\Theta_O \leqq 0.2$) Rh (111).

As is shown in Fig. 2, the mass spectra of methanol decomposition under field-free conditions are dominated by CH_3^+, CO^+, and H_n^+. This result also holds for higher gas pressures up to $\approx 10^{-3}$ Pa, different reaction times, 100 μs $< t_R <$ 10 ms, and temperatures from 300 K up to thermal desorption of the product species. We conclude that the adsorbed layer consists mainly of surface methoxy and product species. If CH_3OH completely decomposed to CO_{ad} and H_{ad} at 298 K, the total hydrogen count, ΣH_n^+ ($n = 1,2$), would be four times as large as the CO^+ intensity. However, if secondary reactions of the product species occur, this argument does not apply. According to Figs. 2 and 3, CO_{ad} is exclusively field desorbed as CO^+ and $RhCO^{2+}$ while Rh-subcarbonyls, $Rh(CO)_x$ ($x = 2,3$), are absent from the mass spectra since the reaction time $t_R = 1$ ms is too short for their formation. On the other hand, the reaction of H_{ad} with O_{ad} to form water cannot be avoided since field desorption of CH_3^+ from CH_3O_{ad} always occurs with high efficiency and leads to continuous supply of O_{ad}. Consequently, the ΣH_n^+ intensities are usually somewhat smaller than expected from considerations of the overall CH_3OH decomposition stoichiometry.

Measurements with rising steady electric fields, F_R, showed that the intensities of CH_3^+ and CH_2O^+ strongly increased while those of H_n^+ and $CO^+ + RhCO^{2+}$ decreased (*11*). This observation was explained by a shift of the chemical equilibrium from the side of the products to the earlier stages, CH_2O_{ad} and CH_3O_{ad}. In the present paper we report on the observation of a kinetic isotope effect during the decomposition of methyl-d_2-alcohol, CHD_2OH, in the pres-

ence of a steady electric field, F_R. Figure 3a and 3b display mass spectra obtained for CH_3OH and CHD_2OH, respectively, at F_R = 4 V/nm. As expected, we find that the prominent peaks of methyl (representing surface methoxy) and formaldehyde species are shifted from 15 to 17, from 30 to 31, and 32 amu, corresponding to CHD_2^+, $CHDO^+$ and CD_2O^+, respectively. The absolute and relative intensities in Fig. 3b are somewhat changed as compared to those in Fig. 3a. This observation is most likely due to slight variations in the kinetics of methanol decomposition when different surface areas of different Rh field emitter tips are probed. Inspection of Fig. 3b reveals that the intensity of CD_2O^+ is larger than that of $CHDO^+$. From the ratio of D to H, 2 : 1, in surface methoxy, CHD_2O_{ad}, an intensity ratio of $[CD_2O^+]/[CHDO^+]$ = 0.5 is expected, because $CHDO^+$ results from D-abstraction which, statistically, should be twice as likely as H-abstraction. The observed ratio of 1.2 indicates a kinetic isotope effect such that C–H bond breaking in adsorbed CHD_2O is more than twice as fast as C–D bond cleavage.

In Figs. 2, 3a, and 3b, the respective ion intensities represent surface concentrations since the pulsed high fields lead to a quantitative desorption after each reaction period, t_R. However, for field strengths $F_D <$ 28 V/nm, accumulation of the surface species may occur because of decreasing probabilities for field desorption. Consequently, reactions in the adsorbed layer may be different and, besides changes of ion intensities, formation of various other surface species is expected.

3.2. Variation of the Desorption Field Strength

The dependence of ionic species and their intensities on the desorption field strength in the absence of a steady electric field was investigated in detail. The results are compiled in Fig. 4. At low fields, $F_D <$ 20 V/nm, the mass spectra contain mainly CH_3^+ ions field desorbed from adsorbed

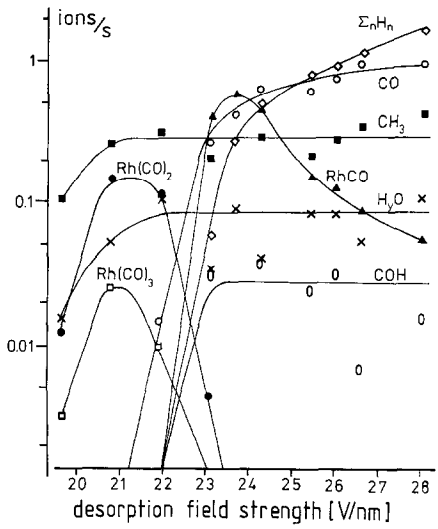

FIG. 4. Variation of the intensities of desorbed species for CH_3OH on rhodium at increasing field strength and zero steady electric field. t_R = 1 ms, T = 298 K, $p = 1.3 \times 10^{-5}$ Pa. (In this measurement, a different tip from that in Fig. 2 was used.)

methoxy. To a smaller extent, also O^+, OH^+, H_2O^+ H_3O^+, (H_yO^+), and Rh-subcarbonyls, $Rh(CO)_x^{2+}$ (x = 2,3), are formed at these low fields. CO^+, $RhCO^{2+}$, CHO^+, and H_n^+ ions appear at higher field strengths of 21–22 V/nm. These different onset fields are determined by different binding energies of the respective neutrals adsorbed on the Rh surface as well as by different ionization energies.

While the intensities of some of the ionic species such as CH_3^+, H_yO^+, CHO^+, CO^+, and H_n^+ level off at increasing field strengths, others, like $Rh(CO)_x^{2+}$ (x = 1–3), pass a maximum and decrease thereafter or even disappear from the mass spectra. Saturation of the intensities also occurs at different field strengths. It is observed that the CH_3^+ and H_yO^+ intensities reach their constant levels at $F_D \approx$ 21 V/nm. The intensity of CHO^+ saturates at $F_D \approx$ 23–24 V/nm while those of CO^+ and H_n^+ tend to level off only at the highest field strengths, $F_D >$ 28 V/nm. Generally, if ion intensities do not increase any more at further raising field strengths, it is to be concluded that the

respective species are quantitatively desorbed by the field pulses. The intensities then reflect the surface concentrations, c_i, in the monitored area. Unfortunately, we cannot give c_i values in terms of fractions of a monolayer since surface-adsorbate stoichiometries and geometries in the mixed overlayer are unknown. However, at a pressure of 1.3×10^{-5} Pa, we do not expect to reach the full monolayer of adsorbed and reacted CH_3OH in times shorter than 10 s. Thus, for the data compiled in Fig. 4, the surface coverage built up during $t_R = 1$ ms does not exceed 10^{-4} of a monolayer.

As can be seen further from Fig. 4, the mass spectra obtained at high fields show mainly H_n^+ and CO^+. Moderate intensities are found for CH_3^+, $RhCO^{2+}$, and H_yO^+. To a small extent, CHO^+ ions are also detected. From the absolute intensities we estimate that nearly 75% of the methanol decomposes whereas about 25% is found in the adsorbed methoxy state (detected as CH_3^+). Methanol was observed to desorb thermally from Rh(111) between 210 and 250 K, the desorption peak temperatures depending on the surface coverage (*10*). The temperature $T = 298$ K in our study is higher, however, the time period, $t_R = 1$ ms, is shorter by orders of magnitude as compared to the time constant of a TPD experiment. Thus, for our experimental conditions, the lifetime of adsorbed methoxy is still long enough. A recent temperature variation measurement displayed decreasing CH_3^+ intensities due to CH_3OH desorption only above $T \approx 360$ K (*19*).

The H_yO^+ ($y = 0$–3) signal follows the same trend as the CH_3^+ intensity but is about four times lower. As mentioned above, H_{ad} (from methanol decomposition) and O_{ad} (from $CH_3O_{ad} \rightarrow CH_3^+$) recombine and desorb as H_yO^+ as well as neutral H_2O. This explanation is in line with the observations that the H_yO^+ ion intensities (i) increase for shorter reaction times than those used in Fig. 4 and (ii) decrease continuously for rising temperatures (*19*).

Carbon monoxide formed in methanol decomposition cannot desorb thermally at $T = 298$ K (*10*). However, it can undergo secondary reactions in the adsorbed layer. This is evidenced by the desorption of $Rh(CO)_x^{2+}$ ($x = 2,3$) ions at low field strengths. We conclude that part of the CO_{ad} is bound in multiple form to a low-coordinated step or kink Rh atom or as di- and tri-carbonyl moieties diffusing over surface terraces. The implications associated with the formation of mobile $Rh(CO)_2$ and $Rh(CO)_3$ molecules are discussed in detail elsewhere (*16*). At high field strengths, $F_D > 23$ V/nm, the concentration of CO_{ad} is drastically lowered by the field pulses so that it is insufficient for Rh-subcarbonyl formation. However, $RhCO^{2+}$ is still observed, because this species is formed by Rh–Rh rather than Rh–CO bond breaking during field desorption of CO_{ad}.

3.3 Deuterium Kinetic Isotope Effect

The mass spectra in Figs. 3a and 3b show that in the presence of a steady electric field, CH_2O^+ can be detected in rather high amounts. Obviously, the electric field decelerates CH_3OH decomposition and stabilizes the intermediate species, CH_3O_{ad} and CH_2O_{ad}. Also, the occurrence of a kinetic isotope effect in the formation of CD_2O^+ and $CHDO^+$ species was pointed out in Fig. 3b. This effect was further investigated by varying the reaction time, the temperature, and the steady electric field. The results of these measurements are shown in Figs. 5a–5c. A high desorption field strength (sum of pulse and steady field) of 29 V/nm was applied in each experiment to ensure quantitative desorption of the adsorbed layer. The reaction time and the temperature were varied in the presence of a steady electric field, $F_R = 4$ V/nm (Figs. 5a and 5b). The absolute intensities of $CHDO^+$ and CD_2O^+ increase linearly with time but the ratio $[CD_2O^+]/[CHDO^+]$ remains fairly constant at 1.2 (Fig. 5a). The temperature dependence of this ratio was studied up to 360 K (Fig. 5b). At higher temperatures, the absolute intensities of the measured species

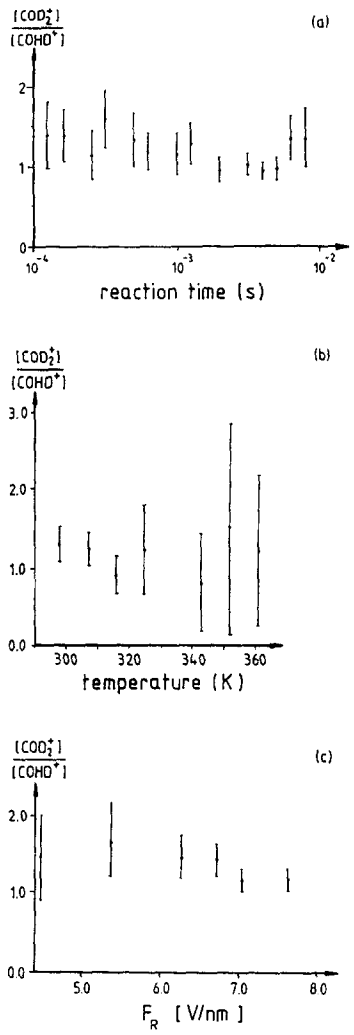

FIG. 5. The ratio $[CH_2O^+]/[CHDO^+]$ plotted as a function of (a) reaction time at constant F_D = 29 V/nm, F_R = 4 V/nm, T = 298 K; (b) temperature at constant F_D = 29 V/nm, F_R = 4 V/nm, t_R = 1 ms; (c) steady electric field, F_R, at constant F_D = 29 V/nm, T = 298 K, t_R = 250 μs.

decreased steeply and could only be restored by further increase of the steady electric field, F_R (*20*). Figure 5c shows the dependence of the $[CD_2O^+]/[CHDO^+]$ ratio on increasing F_R at 298 K and t_R = 0.25 ms. In all three cases, this ratio is about 1.2 which is 2.4 times higher than expected from the statistical abundance of hydrogen/deuterium in CHD_2O_{ad}.

Qualitatively, the observation of a kinetic isotope effect can be explained on the basis of classical transition state theory. An ordinary C–H bond vibration has a zero-point energy which is greater than that of a C–D bond. If that C–H or C–D bond is weakened in the activated complex, then the activation energy of the reaction will be higher for the pathway where a D atom is abstracted than for the one where a H atom is removed. Hence, the rate will be higher for a C–H bond breaking than for a C–D bond cleavage. At T = 300 K, the difference in the activation energies for C–H and C–D bond breaking is about 5 kJ/mol, provided the bond scission in the activated complex is nearly complete. For a typical C–H vibrational frequency, $\upsilon = 8 \times 10^{13}$ s^{-1}, the decomposition rate constant, k, is higher by a factor of 8 for the protonated than for the deuterated compound. Our value, k_{C-H}/k_{C-D} = 2.4 is somewhat smaller but acceptable in view of the many simplifications made by considering only differences in the zero-point energies of C–H and C–D bonds.

3.4. Field Ion Microscopy

Using the technique of FIM, the surface structure before and after long time reaction with methanol was imaged. The method is suited to detect changes in the substrate topography and was successfully applied to the Ni/CO system (*21*). Figure 6a shows a field ion micrograph of a Rh tip, cleaned by field evaporation and imaged in neon at 78 K. The accompanying map (Fig.

FIG. 6. FIM images in neon of Rh tip taken at 78 K before and after exposure to CH_3OH at p = 2 Pa and at 295 K for 10 min; (a) clean surface, imaging field at 35 V/nm; (b) map of dominant planes obtained for the clean surface; (c)–(e) after exposure to CH_3OH at gradually increased imaging fields of 26.7, 32.4, and 33.5 V/nm, respectively.

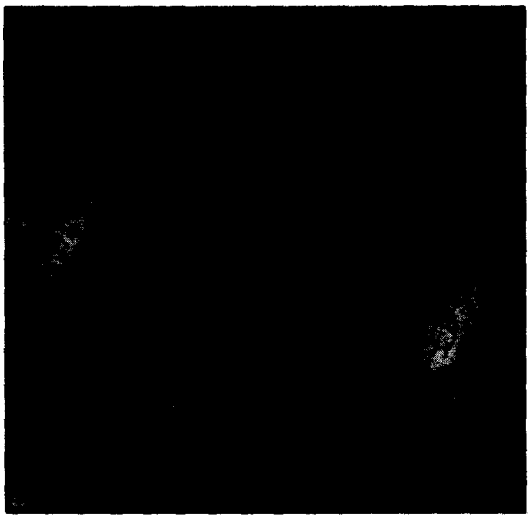

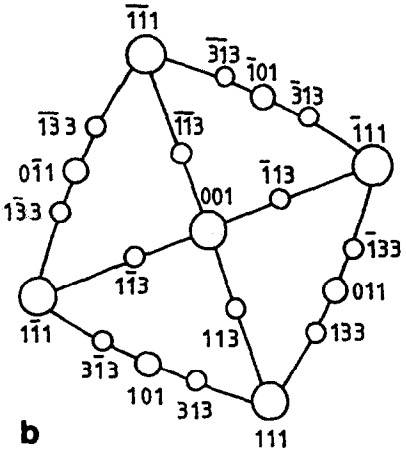
$\bar{1}\bar{1}1$
$\bar{3}\bar{1}3$
$\bar{1}01$
$\bar{3}13$
$\bar{1}\bar{1}3$
$\bar{1}\bar{3}3$
$\bar{1}11$
$0\bar{1}1$
$\bar{1}13$
001
$1\bar{3}3$
$\bar{1}33$
$1\bar{1}3$
011
$1\bar{1}1$
113
133
$3\bar{1}3$
101
313
111
b

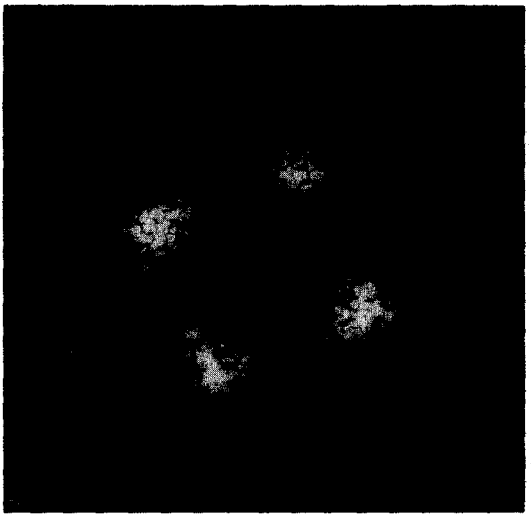

6b) gives the location of dominant low- and high-index planes seen in the images. As is characteristic of a field-evaporated end form high- and low-index planes have rather small diameters. The {001} plane is located in the center of the micrograph and four {111} planes are seen at the periphery. The discrete bright spots in the image represent atoms of the net plane boundaries.

The clean Rh tip was exposed to 2 Pa CH_3OH for 10 min at various temperatures such as 295, 323, 373, and 423 K. Exposure times of 10 min were sufficient in these experiments since at prolonged times only the same results were detected. The FIM images obtained thereafter represent forms attained after adsorption and reaction at the chosen temperature. The ion images were taken at rather low field strengths so that no field evaporation of the substrate occurred. If there were drastic changes in the sizes of the planes and/or the heights between the net planes after the reaction, they could be unambiguously attributed to dissolution of the reactant. Figures 6c–6e show a selection of neon FIM images taken at 78 K after reaction with CH_3OH at 295 K. As the imaging field was adjusted stepwise from small to higher values, surface areas became gradually visible, thus exposing more and more of the surface structure. At moderate fields (Fig. 6c), the {011} planes are seen besides adsorbate molecules which produce extremely bright image spots. At 32.4 V/nm (Fig. 6d), the central (001) and the {111} appear, whereas the {011} are spread over by more bright image spots. Comparison of the diameter of these planes before and after methanol decomposition reaction shows that there are no changes detectable. Also no other dominant higher-index facets were developed. The very slightly reduced top layer of the central (001) plane observed after reaction (Fig. 6d) must be disregarded since such very small changes were also sometimes detected after annealing of the Rh crystal without methanol present. Treatments at higher temperatures lead to the same observations, i.e., no topographical changes can be deduced by FIM following methanol adsorption and decomposition on the Rh surface in the temperature range of 295–423 K.

As was already mentioned above the Rh surface inspected by FIM after methanol decomposition contains remained and still adsorbed species like carbon monoxide, hydrogen, and secondary products, $Rh(CO)_2$ and $Rh(CO)_3$, formed during multiple CO adsorption at Rh surface atoms. These adsorbates may undergo a field activation being essential to show up in the image. Such an activation process can be, for instance, a change of adsorption site of a line up toward a proper direction in the electric field. But these are only secondary effects.

4. DISCUSSION

Methanol decomposition was studied on Rh field emitter surfaces. The apex of a field emitter is nearly a half-sphere with a radius of curvature of ~100 nm and contains a variety of high- and low-index crystal planes. Consequently, the apex can be regarded as a model of a catalyst particle. Field ion microscopy can be used to image the surface planes with atomic resolution before and after a reaction. In this manner, topographical changes of the surface due to the reaction can be visually followed. After methanol decomposition on Rh, the various surface planes were observed to be stable and no corrosion occurred. This is an interesting result since mass spectrometric analysis of the adsorbed layer during CH_3OH decomposition indicates the presence of Rh-subcarbonyls, $Rh(CO)_2$ and $Rh(CO)_3$. These species are formed in secondary reactions of the adsorbed CO evolved from CH_3OH decomposition. In studies of carbonyl formation from CO on Ni field emitter surfaces, a strong reaction and dissolution anisotropy was observed (*21*) and explained by the formation of adsorbed $Ni(CO)_2$ and $Ni(CO)_3$ at Ni kink sites (*22, 23*) and the subsequent ability for diffusion of these moieties on terrace layers. The

absence of structural changes in the CH_3OH decomposition on Rh may be due to the impediment in the detachment of Rh subcarbonyls from kink sites. Such a hindrance could occur because of the simultaneous presence of other species like adsorbed hydrogen, CO, nonreacted CH_xO intermediates, or carbon under conditions of a nearly saturated overlayer. FIM studies at temperatures $T > 423$ K, i.e., under conditions of steady methanol decomposition with fast thermal desorption of the products, CO and H_2, have not yet been performed. However, if CO desorbs, formation of carbonyls becomes unlikely.

While the FIM results refer to the "before and after" state of the catalyst surface, the PFDMS results (Fig. 4) were obtained after a reaction time of 1 ms and using different desorption fields. At low desorption fields, the accumulated layer was not completely desorbed and the species detected are representative of a nearly saturated layer. At high fields, the adsorbed layer was effectively removed by the pulses and thus the species now indicate the extent of the reaction after 1 ms. It is seen that the occurrence of secondary reactions, e.g., the formation of higher-indices $Rh(CO)_x$, is suppressed at high fields. This is because at 298 K the time $t_R = 1$ ms between the field pulses is too short for secondary reactions to occur. In fact, using longer reaction times, $t_R > 10$ ms, $Rh(CO)_x$ were seen, even at high desorption fields, suggesting that the formation of these species is a slow process.

Kinetic measurements. One of the important features of the PFDMS method is its capability to provide kinetic data of a surface reaction even when the products do not desorb thermally. This capability is due to the field pulses which intervene in the ongoing reaction. In this manner a surface reaction can proceed even at temperatures below thermal desorption of the final products. This would hardly be possible with those surface sensitive methods which "observe" rather than "perturbate" the reaction system. On the other hand, PFDMS occasionally exhibits complications due to the high electric field pulses. However, the influence of the electric field on the reaction behavior can be studied by systematically varying a steady electric field, F_R, between the field pulses.

The results presented in this study show that methanol decomposition on Rh occurs rapidly at $T = 298$ K. Substantial parts of the methanol decompose during the reaction time $t_R = 1$ ms, so that the dominating species in the surface layer are CO_{ad} and H_{ad}. No CH_2O^+ and only small amounts of CHO^+ were detected under field-free reaction conditions. The other part of CH_3O_{ad} is field desorbed as CH_3^+ and H_yO^+ ions. Therefore, hydrogen abstraction from CH_3O_{ad} is a rather slow process. This result could be obtained since the accumulation of CO_{ad} and H_{ad} was prevented by the periodically applied field pulses. These product species do not desorb thermally at 298 K so that the reaction would reach a deadlock after $t_R \approx 10$ s at 1.3×10^{-5} Pa.

The CHO species is field desorbed in small amounts only. This species is also formed in the synthesis reaction from mixtures of CO and H_2. Nevertheless, it is unlikely that the occurrence of CHO during methanol decomposition is caused by this back reaction. In this case, we would expect a rapid decrease of the CHO^+ intensity above the thermal desorption temperature of hydrogen. However, such a temperature dependence was not observed in our studies (*11*).

A significant side reaction concerns the formation of water. Unlike the Rh subcarbonyls which are produced by secondary reactions of adsorbed CO, water formation is due to the experimental conditions where the field pulses form CH_3^+ rather than CH_3O^+ from the adsorbed methoxy. The oxygen remaining at the surface reacts effectively with hydrogen and forms water. In fact, this is the same mechanism that was made responsible for the promotion of CH_3OH decomposition on oxygen pre-

covered Rh (111) (*13*). However, deviating from the results obtained by Solymosi *et al.* (*13*), we find only small or even insignificant amounts of CO_2 from a possible surface reaction between O_{ad} and CO_{ad}, due to thermal desorption of CO_2.

Influence of the electric field. A "formaldehyde" species is observed in the presence of a reaction field, F_R, applied during the reaction interval, t_R. This species is not seen under field-free reaction conditions. It is unlikely that CH_2O is formed by field fragmentation of adsorbed methoxy as this process would require the simultaneous cleavage of a Rh–O and a C–H bond. Furthermore, by comparing Fig. 2 with 3a, the CH_2O^+ intensity increases at the expense of CO^+, or the sum of CO^+ and $RhCO^{2+}$ intensities. Thus, the electric field, F_R, seems to shift the reaction equilibrium toward the early intermediate stages of CH_3O and CH_2O. This influence is not surprising since methoxy and carbon monoxide are adsorbed with dipole moments of just opposite signs. While CO adsorption on metal surfaces generally leads to an increase of the work function, the opposite behavior is found for CH_3O_{ad} on Rh (111) (*13*). During the decomposition of the methoxy, the binding mode must change from Rh–O to Rh–C in adsorbed CO. A two-point adsorption of CH_2O_{ad} involving both Rh–O and Rh–C bonds can be envisaged as a hypothesis of understanding how hydrogen abstraction from methoxy occurs. In the presence of the electric field, F_R, the upright orientation, Rh–O–CH_x, is energetically favored because of the interaction of its dipole moment with the field. We therefore propose the model that CH_2O_{ad} is kept upright by F_R and, thus, its decomposition is inhibited. The observation that at elevated temperatures the stabilization of CH_2O_{ad} can be achieved with higher fields, F_R, only (*20*), further supports this model.

From our results, methanol decomposition on stepped Rh surfaces occurs by stepwise hydrogen abstraction from a methoxy species formed initially during dissociative CH_3OH adsorption:

$$CH_3O_{ad} \rightarrow CH_2O_{ad} + H_{ad} \rightarrow CHO_{ad} + 2H_{ad} \rightarrow CO_{ad} + 3H_{ad}.$$

Under our experimental conditions ($t_R < 10^{-2}$ s, $p < 1.3 \times 10^{-5}$ Pa), the surface coverage is always below 1% of a monolayer. Thus, the reaction steps occur unimolecularly with little or no interaction between the decomposing molecule and species at adjacent sites.

Since the CH_3O_{ad} concentration is always much higher (at $F_R = 0$) than the CH_2O_{ad} and CHO_{ad} concentrations we conclude that the reaction step

$$CH_3O_{ad} \rightarrow CH_2O_{ad} + H_{ad}$$

is slow. This is further supported by the occurrence of a kinetic isotope effect when using methyl-d_2-alcohol, CHD_2OH, instead of CH_3OH. Under the influence of a steady electric field which serves to stabilize the "formaldehyde" intermediate, an intensity ratio $[CD_2O^+]/[CHDO^+] \approx 1.2$ is found which is 2.4 times higher than expected from the amount of hydrogen in CHD_2O_{ad}. The ratio was observed to be nearly independent of reaction time, surface temperature, and steady electric field. The importance of the C–H bond scission in adsorbed methoxy was also found by other authors in reaction studies on Ni low-index single crystal surfaces (*24–27*).

ACKNOWLEDGMENT

Financial support by Sonderforschungsbereich (SFB 6/81) is gratefully acknowledged.

REFERENCES

1. Bhasin, M. M., and O'Connor, G. L., Belgian Patent 824,822 (1975).
2. Poutsma, M. L., Elek, L. F., Ibarbia, P. A., Risch, A. P., and Rabo, J. A., *J. Catal.* **52,** 157 (1978).
3. Christmann, K., and Demuth, J. E., *J. Chem. Phys.* **76,** 6308 (1982); **76,** 6318 (1982).
4. Gates, J. A., and Kesmodel, L. L., *J. Catal.* **83,** 437 (1983).

5. Kok, G. A., Noordermeer, A., and Nieuwenhuys, B. E., *Surf. Sci.* **135,** 65 (1983).
6. Hrbek, J., de Paola, R. A., and Hoffmann, F. M., *J. Chem. Phys.* **81,** 2818 (1984).
7. Wachs, J. E., and Madix, R. J., *Surf. Sci.* **76,** 531 (1978).
8. Sexton, B. A., *Surf. Sci.* **102,** 271 (1981).
9. Ehlers, D. H., Spitzer, A., and Lüth, H., *Surf. Sci.* **160,** 57 (1985).
10. Solymosi, F., Berkó, A., and Tarnóczi, T. I., *Surf. Sci.* **141,** 533 (1984).
11. Kruse, N., Chuah, G.-K., Abend, G., Cocke, D. L., and Block, J. H., *Surf. Sci.* **189/190,** 832 (1987).
12. Berkó, A., Tarnóczi, T. I., and Solymosi, F., *Surf. Sci.* **189/190,** 238 (1987).
13. Solymosi, F., Berkó, A., and Tarnóczi, T. I., *J. Phys. Chem.* **88,** 6170 (1984).
14. Block, J. H., and Czanderna, A. W., *in* "Methods of Surface Analysis" (Czanderna, A. W., Ed.), Vol. 1, p. 379, Methods and Phenomena I: Their Applications in Science and Technology. Elsevier, Amsterdam, 1975.
15. Kruse, N., Abend, G., and Block, J. H., *J. Chem. Phys.* **88(2),** 1307 (1988).
16. Kruse, N., Abend, G., and Block, J. H., *J. Chem. Phys.*, in press.
17. Gurney, B. A., and Ho, W., *J. Chem. Phys.* **87(9),** 5562 (1987).
18. Zinck, J. J., and Weinberg, W. H., *J. Vac. Sci. Technol.* **17,** 188 (1980).
19. Chuah, G.-K., Kruse, N., Abend, G., and Block, J. H., to be published.
20. Chuah, G.-K., Kruse, N., Block, J. H., and Abend, G., *J. Phys.* **48,** C6-493 (1987).
21. Schmidt, W. A., Block, J. H., and Becker, K. A., *Surf. Sci.* **122,** 409 (1982).
22. Liang, D. B., Abend, G., Block, J. H., and Kruse, N., *Surf. Sci.* **126,** 392 (1983).
23. Kruse, N., Abend, G., Drachsel, W., and Block, J. H., *in* "Proceedings, 8th Int. Congress on Catalysis" (DECHEMA Berlin/FRG, Ed.), Vol. 3, p. 105. Verlag Chemie, Weinheim, 1984.
24. Richter, L. J., and Ho, W., *J. Vac. Sci. Technol. A* **3,** 1549 (1985).
25. Baudais, F. L., Borschke, A. J., Fedyk, J. D., and Dignam, M., J., *Surf. Sci.* **100,** 210 (1980).
26. Gates, S. M., Russell, J. N., Jr., and Yates, J. T., Jr., *Surf. Sci.* **146,** 199 (1980).
27. Gates, S. M., Russell, J. N., Jr., and Yates, J. T., Jr., *J. Catal.* **92,** 25 (1982).